



ICOVP, 13th International Conference on Vibration Problems
29th November – 2nd December, 2017, Indian Institute of Technology Guwahati, INDIA

A SIMPLIFIED IMPACT DAMPING MODEL FOR HONEYCOMB SANDWICH USING DISCRETE ELEMENT METHOD AND EXPERIMENTAL DATA

N. AHMAD^{PR,CR}, R. RANGANATH

ISRO Satellite Centre, Old airport road, Bangalore, 560017, India
nazeer@isac.gov.in, rrrr@isac.gov.in

A. GHOSAL

Indian Institute of Science, Bangalore 560012, India
asitava@mecheng.iisc.ernet.in

Abstract. Honeycomb sandwich laminates with aluminum and carbon fiber reinforce polymer (CFRP) face – sheets are widely used in spacecraft structures and aerospace industries. The damping behavior of such structures are reported to improve when the empty cells of the honeycomb core is filled with damping particles. The discrete-element-method (DEM) has been successfully used and found to give reasonably accurate estimate of the impact damping. The DEM is based on Newtonian mechanics where equation of motion of each particle is established by considering the contact forces and moments from the surrounding particles and boundary contacts or from any other source. The motion of each particle and its interaction with surrounding boundaries is tracked and energy dissipation through impact and friction is computed. The use of DEM for real structure where number of particles are of order 10^8 or more is inefficient and impractical to perform optimization. In this paper a damping model dissipating equivalent energy is presented for a system consisting of small honeycomb sandwich coupon filled with damping particles and has resonance frequencies beyond the bandwidth of the model. The coupon is subjected to a range of harmonic excitations (varying frequency and amplitude). The energy dissipated by the damping particles filled are estimated by DEM. The particle-particle and particle-wall impact is modeled using Hertz's non-linear dissipative contact model for normal component and Coulomb's laws of friction for tangential component. Then the parameters of the equivalent damper are obtained which dissipates same energy. The damping model presented incorporates the effect of fill fraction, particle size and material as well as the amplitude and frequency of excitation. The comparison of the DEM model for some the load cases is done with the experimental data showing reasonably good agreement. The model presented could be readily incorporated in the FEM model like zero-stiffness proof-mass actuator and effect of impact damping can be studied without actually solving the equations of motion of the damping particles.

Keywords. Impact damping, discrete element method, Honeycomb sandwich, granular damping particles, passive vibration isolation, spacecraft structure

1. Introduction

Sandwich composites with honeycomb core are widely used in aerospace industries owing to its light weight and excellent mechanical properties. However, in general, a honeycomb sandwich composite possesses very small, less than 2%, inherent structural damping which results in excessive resonance responses endangering the integrity of the structure and also the subsystems mounted on it. The damping characteristic of honeycomb is reported to

improve when granular particles are inserted in the empty cells of the honeycomb core [1]. This technique of enhancing damping is called particle impact damping. A particle impact damper (PID) is extremely simple to implement, insensitive to environment, low cost and effective over wide temperature and frequency range. A particle impact damper dissipates the energy of a vibrating system by impact and friction. The energy dissipation mechanism in PID is highly nonlinear and depends on a host of parameters: size, shape, number and material of the particles; enclosure relative geometry and material; mass ratio; volumetric packing fraction; location of PD with respect to structural mode; and the level of response. The dissipation of energy takes place mainly through inter-particle and particle-wall impact and friction. The dominant mode of dissipation depends on the relative proportion of different parameters. It is extremely difficult to evolve a model to capture the entire interactions taking place. There are many modelling techniques reported in literature for particle impact damping problem [2-5]. One of the method that is widely used in the particle assemblage simulation is discrete element method (DEM) [6]. The DEM alone takes into account the particle to particle level interaction enabling to study the dependence of energy dissipation on large number of parameters. The DEM is based on Newtonian mechanics where equation of motion of each particle is established by considering the contact forces and moments from the surrounding particles and boundary contacts or from any other source. The motion of each particle and its interaction with surrounding boundaries is tracked. For the larger problems where millions of particle motion is required to be solved coupled with the dynamics of the structure, the DEM becomes inefficient. Generally, honeycomb sandwich panels used are large and thus number of damping particle required to effect the damping characteristic is huge. Thus, the use of DEM is computationally very expensive. Therefore, in this work DEM is applied on a honeycomb sandwich coupon of smaller size filled with damping particle. The coupon is subjected to vibration loads and the energy dissipated is estimated and further its dependence on the other parameter is studied. An equivalent damper which dissipates same amount of energy per cycle is estimated which could be readily integrated like a proof mass actuator with enabling prediction of structural responses without solving.

2. Mathematical Formulation

A small square shaped coupon of the honeycomb sandwich, shown in Figure 1, is considered for the assessing the dissipation of energy by damping particles. The coupon is of 100mm x 100mm x 25.4mm dimension. The coupon is very stiff; a normal mode analysis with free-free boundary condition shows that the first natural frequency is at 6235.2 Hz and corresponding mode shape is shown in Figure 2. In this study where we intend to study the damping behavior up to 1000 Hz. The coupon is assumed to be rigid and therefore, cells of the honeycomb do not rotate and undergo deformation. The equations of the cell walls with respect to a local coordinate system, which is at the geometric center of the cell with axis parallel to the global axis, is shown in Figure 1, is given by Eqs (1). The x-axis of global coordinate system is along the L-direction of the core and y-axis is along the W-direction of the core.

$$\begin{aligned}
 \bar{z} \pm \frac{h}{2} &= 0 \\
 \bar{y} \pm \frac{\sqrt{3}}{2} R &= 0 \\
 \bar{x} + \frac{\bar{y}}{\sqrt{3}} \pm R &= 0 \\
 \bar{x} - \frac{\bar{y}}{\sqrt{3}} \pm R &= 0
 \end{aligned} \tag{1}$$

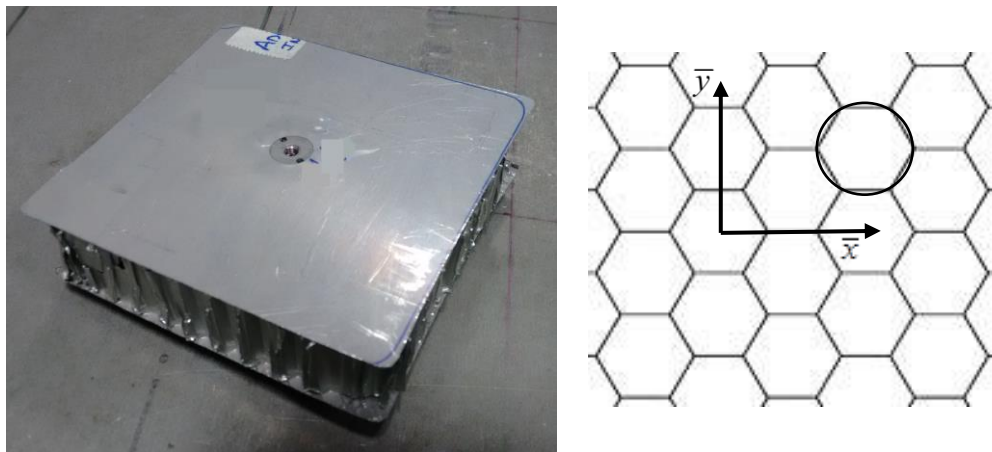


Figure.1. Honeycomb coupon and axis definition

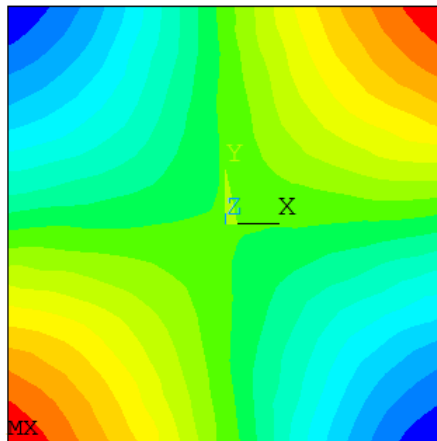


Figure.2. First mode of the coupon

The damping particles are constrained to move inside the cell as shown in Figure 3 when coupon is vibrated. The damping particles in the cells, collide and rub with the walls of the cells and face-sheets as well as between themselves. The rubbing and collision results in momentum transfer and energy dissipation. An impact results in normal and tangential forces, the normal force is modelled by Hertz's nonlinear dissipative contact model defined as.

$$\mathbf{f}_{ij}^n = -\left(k_n (\delta_{ij}^n)^{3/2} + \alpha \sqrt{m_{ij}^* k_n} (\delta_{ij}^n)^{1/4} \delta_{ij}^x\right) \mathbf{n}_{ij} \quad (2)$$

where δ_{ij}^n is the normal relative velocity of the center of particle i with respect to the center of particle j and α is the damping constant and a nonlinear function of the normal coefficient of restitution e_n [7], defined as.

$$\alpha = -\ln(e_n) \sqrt{\frac{5}{\ln(e_n)^2 + \pi^2}} \quad (3)$$

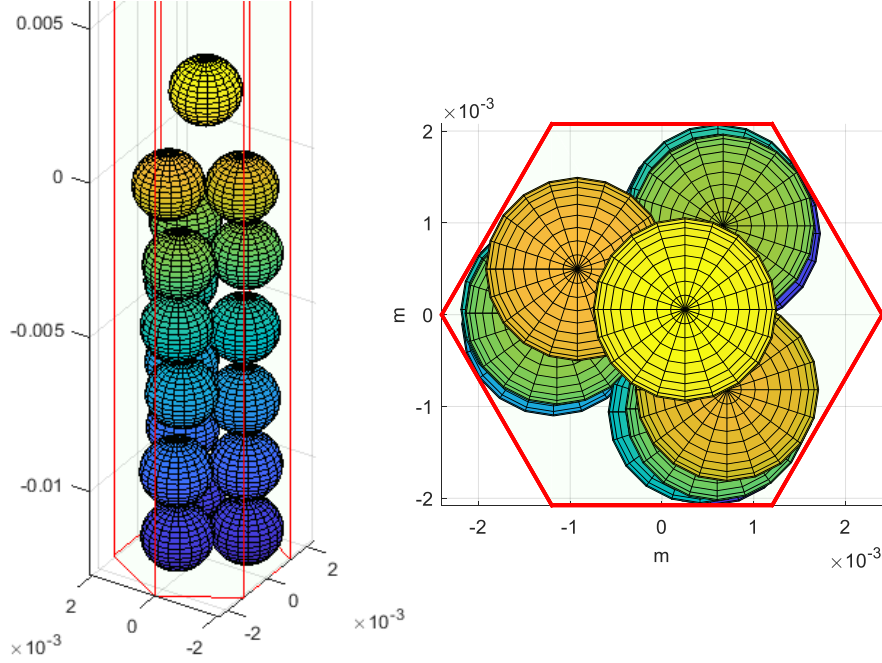


Figure.3. Motion of damping particles in a cell

The elastic Hertz's constant k_n for spherical impacting bodies and sphere-plan wall is given in [8], and the equivalent mass m_{ij}^* in Eq. (2) is defined as

$$m_{ij}^* = \frac{m_i m_j}{m_i + m_j} \quad (4)$$

The tangential contact force is modelled the coulomb's law of sliding friction [8] that is easiest to implement and most efficient among all the models for tangential force component computation in a contact process, given as

$$\mathbf{f}_{ij}^t = -\mu \left| \mathbf{f}_{ij}^n \right| \frac{\mathbf{V}_{ij}^t}{\left| \mathbf{V}_{ij}^t \right|} \quad (5)$$

where μ is the coefficient of friction and \mathbf{V}_{ij}^t is the relative tangential velocity of contact points. The change in the velocity and evolution of the forces/moments during an oblique contact process is given in Figures 4 and 5. Figures 4a-d present the velocity and forces

moments when a damping particle collides with an velocity of $[0 \ 0.5 \ -0.1]$ m/s to the plane, $z = -h/2$. Figures 4c and 4d show the effect of nonlinear dissipative terms present in the expression for normal force, due to this dissipative term the relative velocity is reaching to zero well before the end of the contact process which can be seen as small loop at the end of contact process.

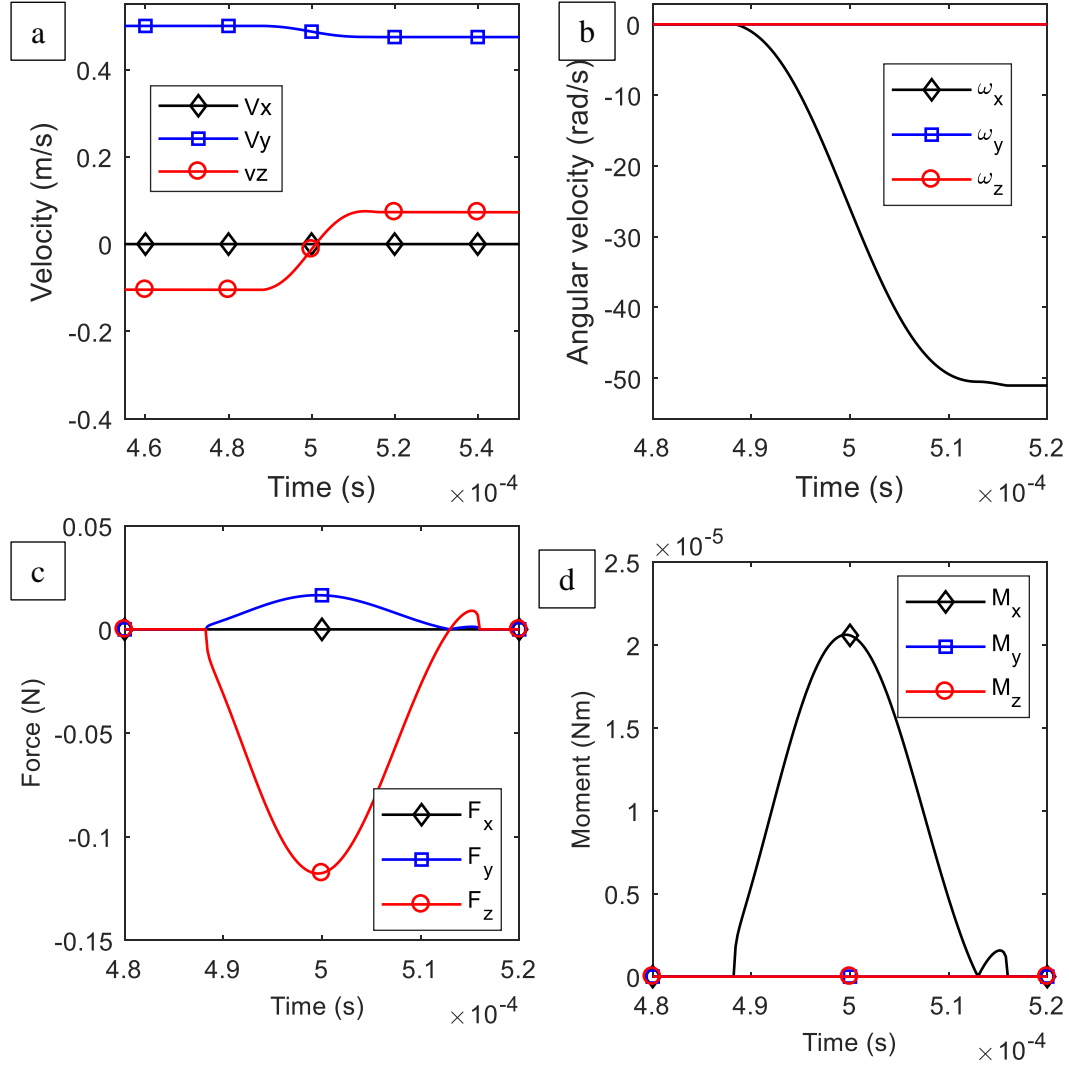


Figure.4. Change in velocities of a particle colliding walls of the cells

The pre and post collision velocity and force distributions of the same damping particle colliding again with plan: $\bar{y} - \sqrt{3}/2R = 0$ is given in Figures 5a-d. As it is known that the Coulomb's model of friction force gives grossly erroneous results of post impact dynamics when the angle of incidence is small (less than a critical value that depends on material properties of impacting bodies, for ordinary material it is around 30 degree, see [8]). The tangential force oscillates due to change in the direction of the tangential velocity this phenomenon is clearly visible in time-tangential force plot in Figure 5d. It captures only gross-sliding and rolling phases and fails to predict the negative bounce for certain angles of incidence. However due to its simplicity and speed it is extensively used by researcher in vibration problems.

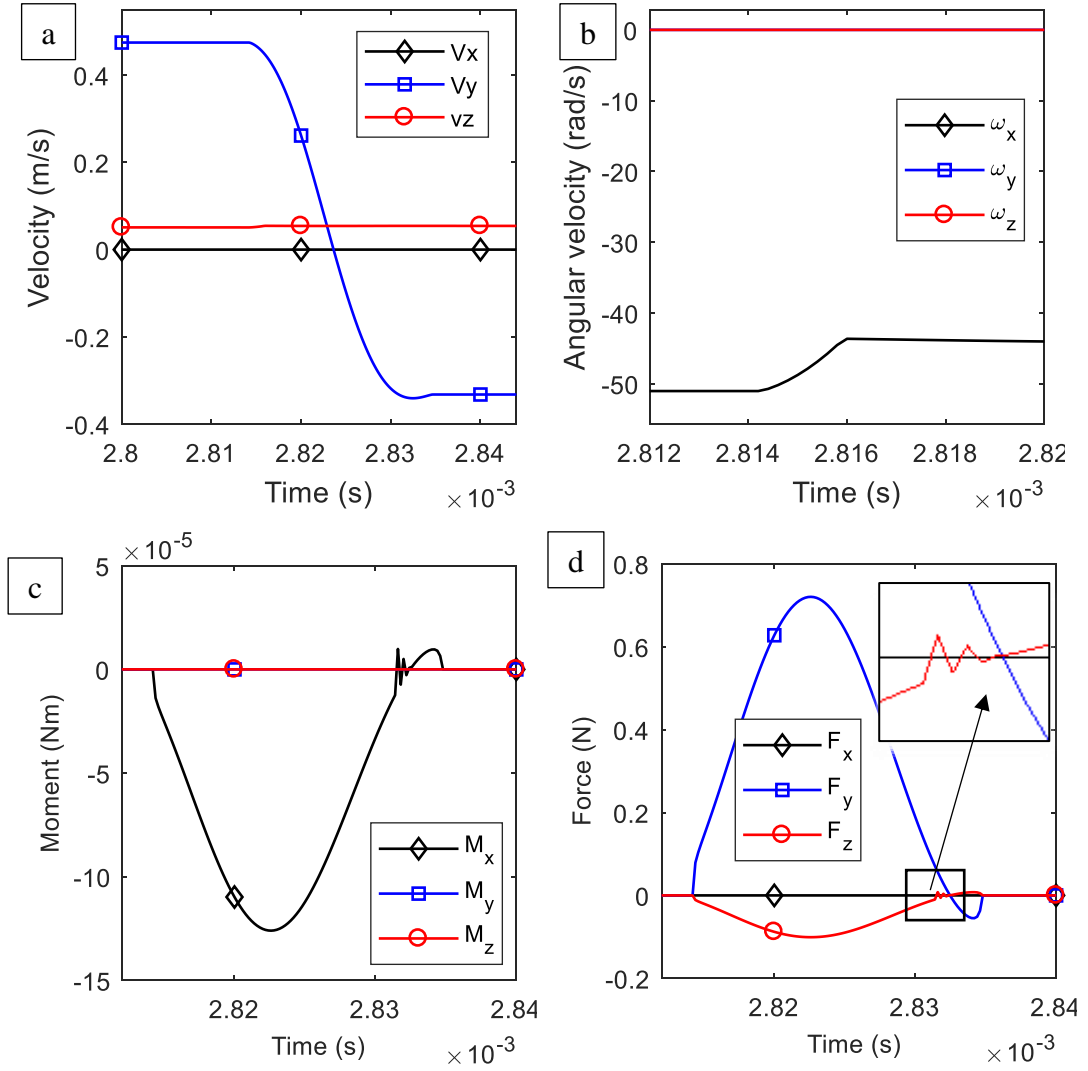


Figure.5. Change in velocities of a particle colliding walls of the cells (2^{nd} collision)

The motion of the DP in the cell can be described by the force and moment equations as

$$\begin{aligned}
 m_{pi} \dot{\mathbf{p}}_i &= -m_{pi} \mathbf{g} + \sum_{j=1}^{n_1} \mathbf{f}_{ij} + \sum_{w=1}^{n_2} \mathbf{f}_{iw} \\
 \mathbf{I}_i \dot{\boldsymbol{\Phi}}_i &= \sum_{j=1}^{n_1} \left(r_i - \frac{\delta_{ij}}{2} \right) \mathbf{n}_{ij} \times \mathbf{f}_{ij} + \sum_{j=1}^{n_2} (r_i - \delta_{iw}) \mathbf{n}_{iw} \times \mathbf{f}_{iw}
 \end{aligned} \tag{6}$$

where m_{pi} , r_i , and \mathbf{I}_i are the mass, radius and mass moment of inertia of the particle i , respectively; \mathbf{p}_i is the position vector of the centre of mass and $\boldsymbol{\Phi}_i$ the angular displacement of the particle i . The unit vectors \mathbf{n}_{ij} and \mathbf{n}_{iw} point from the centre of the particle i towards the centre of the particle j and towards the point of contact with cell wall. The acceleration due to gravity is represented by \mathbf{g} and \mathbf{f}_{ij} and \mathbf{f}_{iw} are the forces on particle i due to interaction of particle j and by the wall of the cell, respectively. The normal relative displacements of the centre of mass of the particle i with respect to the particle j when they are in contact

with each other or with the wall are represented by, δ_{ij} and δ_{iw} , respectively. The DEM formulation assumes that the motion of any particle is affected by its immediate neighborhood contacts only. This implies that the time step chosen to integrate the equations of motion should be small enough so that the disturbance does not propagate beyond its immediate neighbor in single step and it must at least an order less than the contact period. In this work a time step 2×10^{-6} s is used.

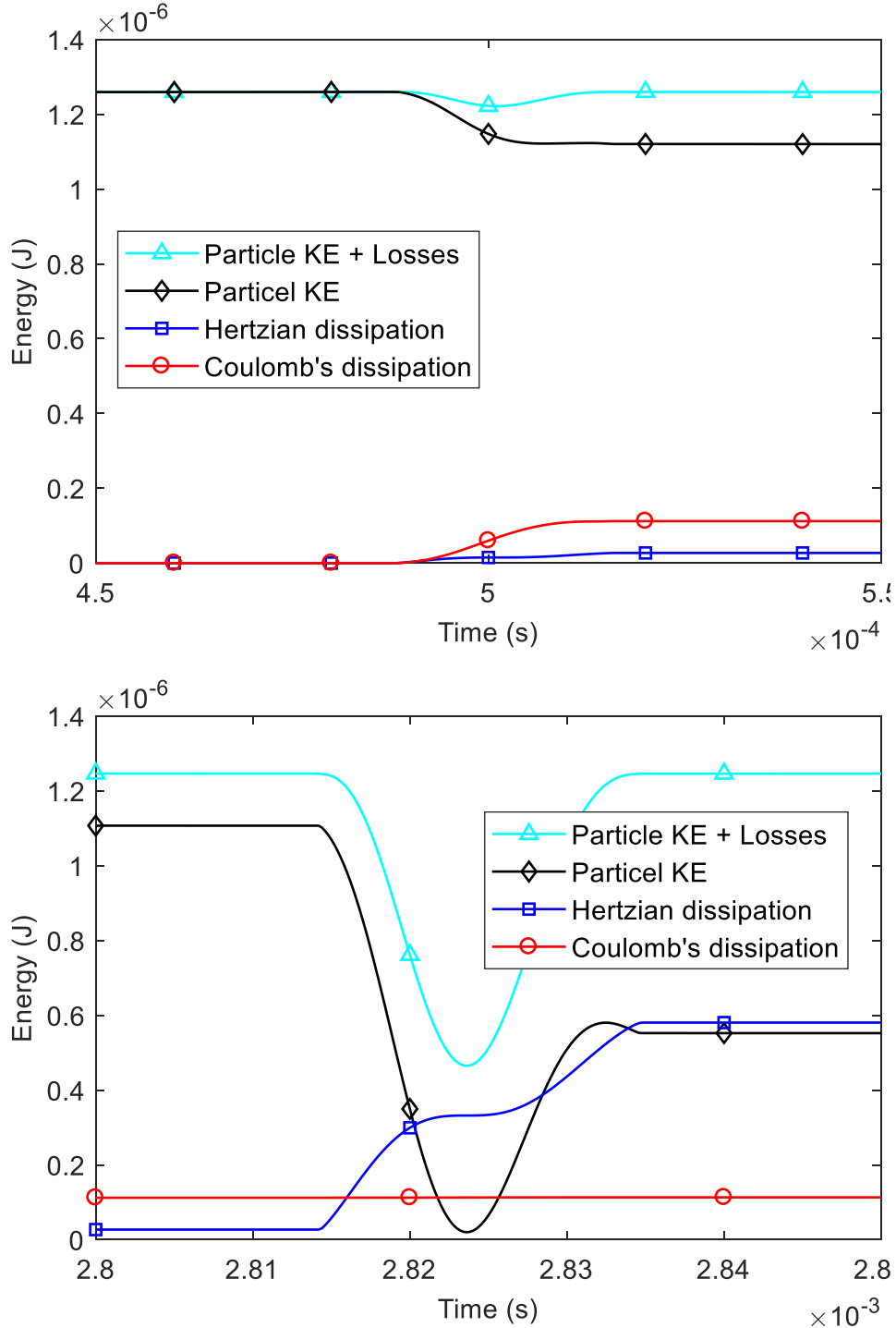


Figure.6. Energy dissipation prediction by equation 7 (1st and 2nd collision)

The energy dissipated per unit area by the contact forces during impact as result of vibration can be written as

$$E_d = \frac{\sum_{k=1}^{N_c} \int_0^{t_c} \left(\alpha \sqrt{m_{ij}^* k_n} \delta^{1/4} \dot{\delta}_{ij} + f_{ij}^t \dot{\delta}_{ij} \right) dt}{A} \quad (7)$$

Where t_c is the contact duration, N_c is the number of contacts, A is the area of the coupon and E_d is the energy dissipated. The energy dissipated by Hertz's and Coulomb's forces for a single particle collision described above in two events are given in Figure 5.

3. Criterion for PID performance

The PID dissipates energy by Collision and friction which results in damping effect on structure as it takes energy from the structures. As the process being highly nonlinear the criterion for performance assessment should hold for harmonic as well as transient vibrations. Specific damping capacity (SDC) is one such parameter which is used for assessment of performance of a PID [9]. It is defined as

$$\eta = \frac{\Delta E}{E} \quad (8)$$

Where ΔE is the kinetic energy converted into heat during one cycle of vibration, and E is the maximum kinetic energy during the cycle. If the structure is subjected to harmonic excitation of constant acceleration amplitude, then

$$\Delta E = E_d \quad (9)$$

And E is given by

$$E = \frac{1}{2\omega^2} m_c a^2 \quad (10)$$

The specific damping capacity is related to the loss factor as $\eta/2\pi$ and to the linear damping as $-\ln(1-\eta)/4\pi$.

4. Specific damping computation and experimental validation

The specific damping capacity computation is performed for the acrylic damping particles. The properties of the damping particles are given in Table 1 and the properties of coupon is given in Table 2. The specific damping capacity is studied with respect to excitation acceleration level, frequency of excitation, and fill fraction as these are the parameters on which SDC is strongly dependent. It is reported in literature that the density of the DP affects the performance but in context of the honeycomb structures where it cannot be loaded with metallic particles as it will drastically increase the weight of the structure nullifying the advantage it offers due to its light weight. Therefore, in this study, light particle like acrylic is used and study with respect to density of DP is ignored.

Table.1. Properties of damping particles

Properties	Units	Aluminum	Acrylic
Radius	mm	1	1.25
Density	kg/m ³	2850	1180
Young's modulus	N/m ²	70 x 10 ⁹	2.84 x 10 ⁹
Poisson's ratio	-	0.33	0.402
Material pairs		Coefficient of sliding friction	Normal restitution coefficient
Aluminium – aluminium	-	0.50	0.85
Acrylic – acrylic	-	0.096	0.70
Acrylic – aluminium	-	0.14	0.70

Table.2. Properties of honeycomb coupon

Properties	Units	Face-sheet (AA 2024 T3)	Honeycomb core (CR 3/16-5056-0.0007-P-32)
Thickness	mm	0.25	25.4
Density	kg/m ³	2800	32.1
Young's modulus	N/m ²	72 x 10 ⁹	$E_{xx} = E_{yy} = E_{zz} = 10000$
Poisson's ratio		0.33	$\nu_{xy} = \nu_{yz} = \nu_{xz} = 0.3$
Shear modulus	N/m ²	-	$G_{xy} = 10000$ $G_{yz} = 0.89 \times 10^8$ $G_{xz} = 1.85 \times 10^8$
Diameter of inscribing circle of hexagonal cell	mm	-	4.76

1.1. Experimental setup

The coupon was excited by a modal shaker (make: M B Dynamics, model: 2050A, Force rating: 100N) fixed at center of the coupon. A high sensitivity impedance head (make: PCB, model: 288D01) for measuring the input acceleration and force sensor was attached at the top of the stinger connecting the modal shaker to the coupon. For measurement of velocity a PDV-100 Portable Digital Vibrometer was used. A 32 channel data acquisition system (DAS) from LMS was used for data acquisition and LMS Test Lab software was used for data processing. The setup is shown in Figure 7.

1.2. Computing the loss factor using experimental data

The loss factor can be computed from the direct measurement of velocity by laser vibrometer and the input force sensor fixed between the stinger and coupon. Let the $f(t)$ and $v(t)$ represents the instantaneous signals from the from force sensor and laser vibrometer, respectively, then the complex power P_c can be expressed as [10, 11]

$$P_c = \frac{1}{T} \int_0^T \left(\sum_{n=0}^{\infty} f_n e^{j(n\omega t - \phi_f)} \right) \left(\sum_m v_m e^{j(m\omega t - \phi_v)} \right) \quad (11)$$

The loss factor can be obtained from the complex power P_c as it is the ratio of the real and imaginary parts of the complex power given by Eqn. (11). The loss factor can be related to SDC as discussed in section 3. The SDC obtained for some of the load cases is given Table 3. Three levels of harmonic input acceleration of constant amplitudes of [1 5 10]g at

frequency points [50 100 500 1000] Hz for varying fill fractions are computed using the DEM and results are given in Table 3 along with measured values. The coupon contains 441 cells and each cell can accommodate a maximum of 36 damping particles (100% fill fraction). As the DEM takes 12 to 16 hrs of computational time for each load case, and SDC depends on range of parameters predominantly on fill fraction frequency of excitation and input acceleration amplitude, a multivariate interpolation function is proposed. The interpolating function is obtained using the data given in the Table 3 and the values of SDC at intermediate data points are generated using the interpolation function.



Figure.7. Experimental setup

Table.3. SDC

Frequency (Hz)	Acceleration (g)	Packing ratio	Specific damping capacity Method (DEM)	Experimental
50	1	25	1.5702e-4	
		50	0.0018	0.10
		75	0.0051	
		90	0.0089	
	5	25	0.2210	
		50	0.1856	0.23
		75	0.2904	
		90	0.3490	
	10	25	0.1150	
		50	0.2783	0.31
		75	0.3914	
		90	0.4832	
100	1	25	2.9705e-4	
		50	0.0032	0.01
		75	0.0109	
		90	0.0195	
	5	25	0.1836	
		50	0.1891	0.21
		75	0.3158	
		90	0.3190	
	10	25	0.1211	
		50	0.2648	0.32
		75	0.3849	
		90	0.4321	
500	1	25	0.0034	
		50	0.1443	0.22
		75	0.4963	
		90	0.6503	
	5	25	0.1965	
		50	0.5417	0.65
		75	0.8044	
		90	0.8359	
	10	25	0.0975	
		50	0.2770	0.35
		75	0.4145	
		90	0.4756	
1000	1	25	0.0505	
		50	0.6138	0.71
		75	0.8078	
		90	0.8010	
	5	25	0.1968	
		50	0.5612	0.63
		75	0.8720	
		90	0.8843	
	10	25	0.0911	
		50	0.2886	0.30
		75	0.4444	
		90	0.5305	

1.3. Variation of SDC with input acceleration amplitudes

Figures 8-12 show the variation of SDC with respect to input acceleration levels at fill fractions varied from 25%, 50, 75% and 90%, respectively. For all the fill fractions SDC increases as acceleration level increased up to 5g and thereafter it is seen decreasing till 10g. The levels computed using DEM and interpolated is shown in the legend. For low fill fractions a lower value of SDC can be attributed to lesser number of particles in the cell and thus less number of collision and therefore smaller values of SDC. The value of SDC appears almost constant in frequency range of study. However, for the fill fractions 50%-90%, SDC increased up to 500Hz and thereafter remains nearly constant.

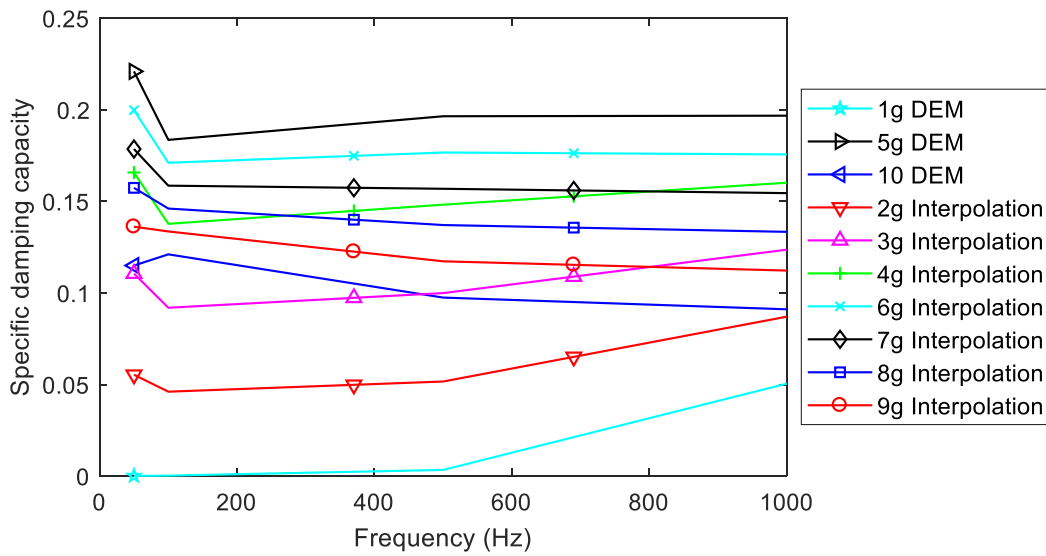


Figure.8. SDC at 25% fill fraction

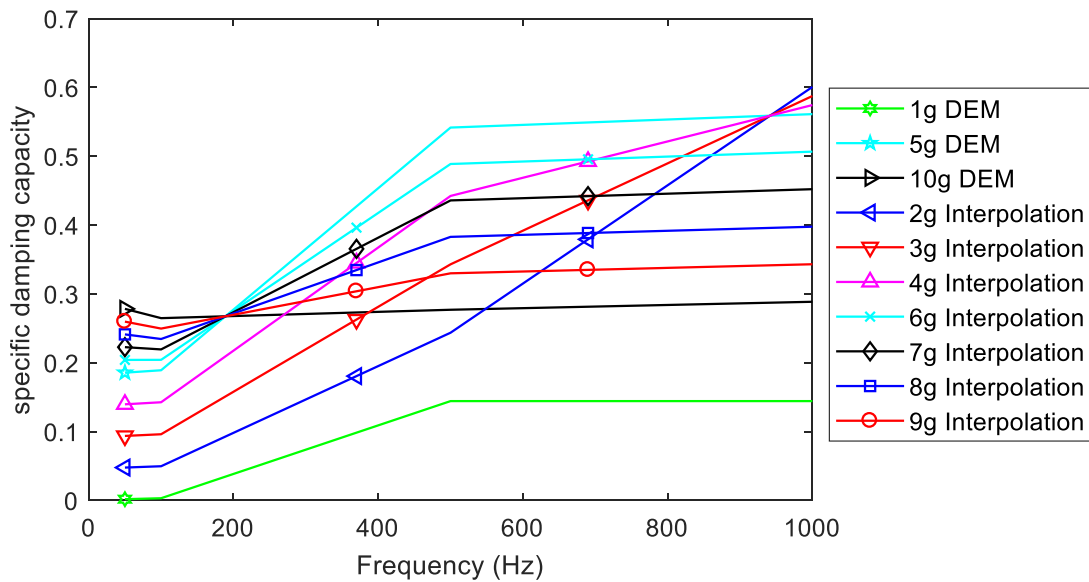


Figure.9. SDC at 50% fill fraction

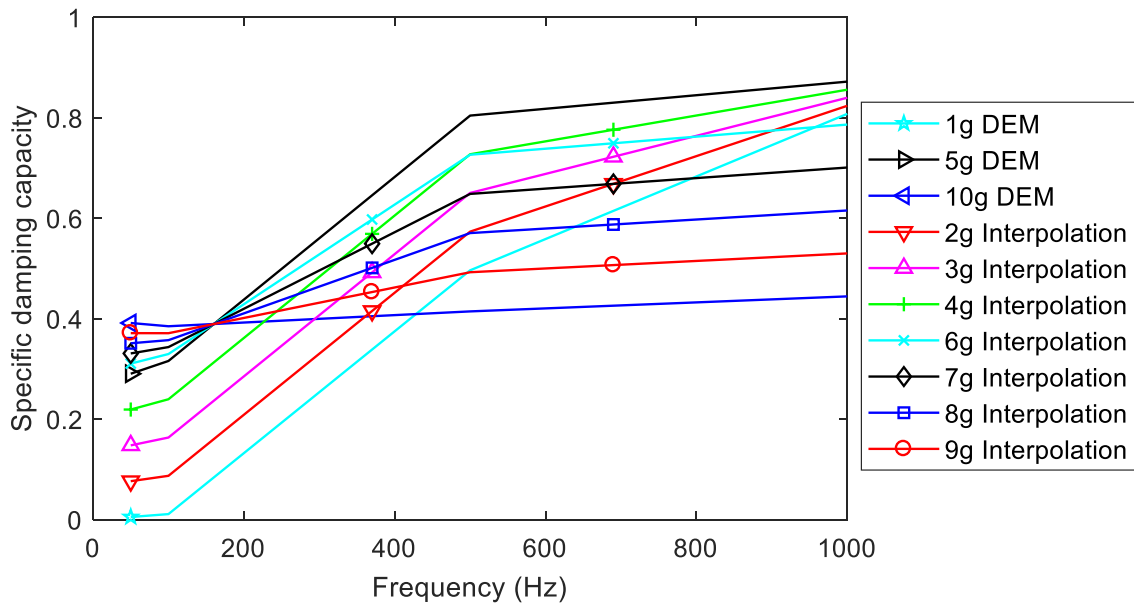


Figure.10. SDC at 75% fill fraction

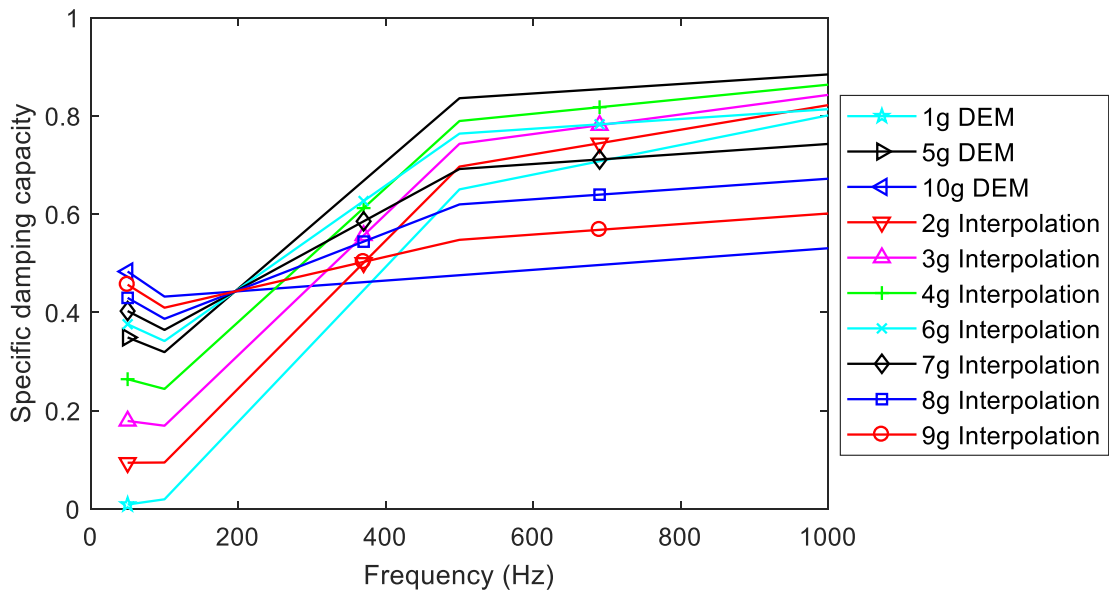


Figure.11.SDC at 90% fill fraction

1.4. Variation of SDC with varying fill fraction

Figures 12-14 present the variation of SDC with respect frequency when amplitude of harmonic input acceleration is kept constant and packing ratio is varied. The SDC is seen increasing with respect to frequency at lower acceleration levels for all fill fractions. However, the rate of increase with respect to acceleration level decreases as acceleration increase. At an acceleration level of 10g, SDC appears to be independent of frequency. The likely reason for such behavior could be the fact that particles remains most of the time in the cavity space and colliding less frequently with the structure.

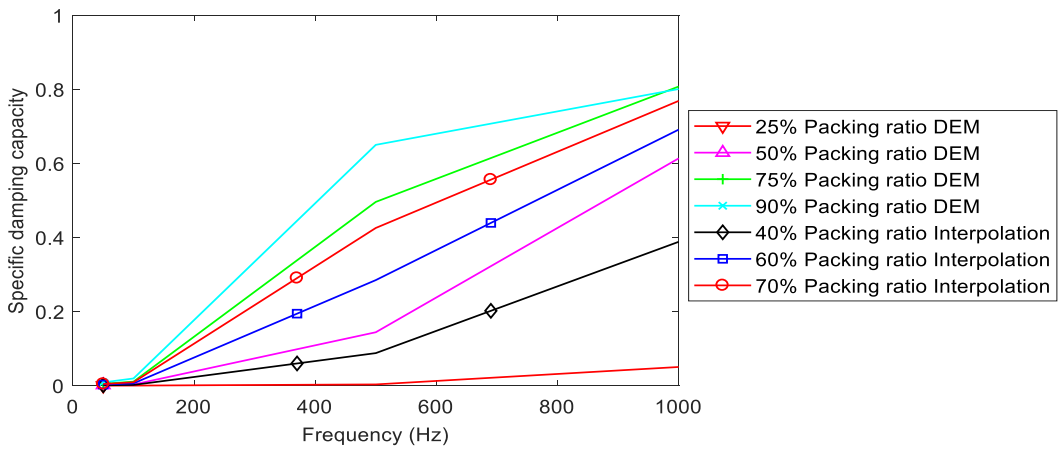


Figure.12. SDC at 1g acceleration level

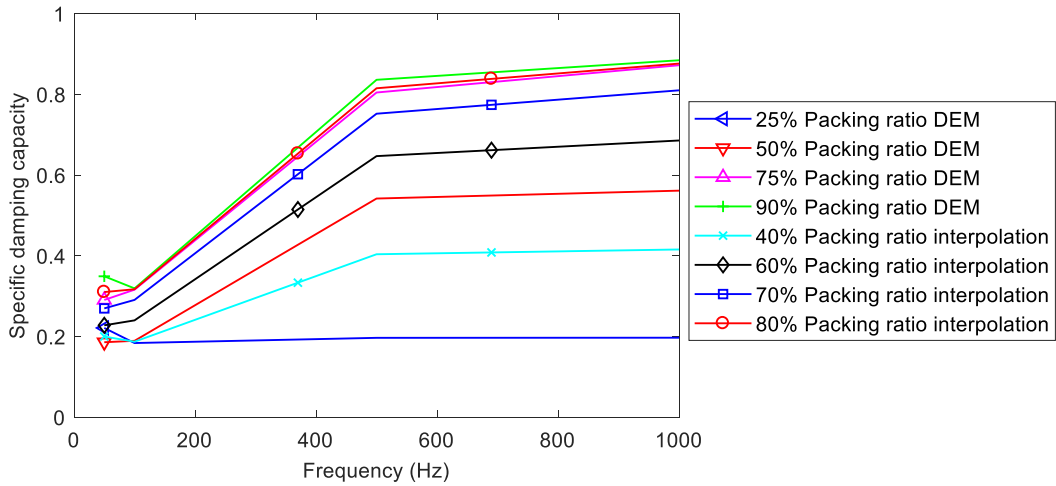


Figure.13. SDC at 5g acceleration level

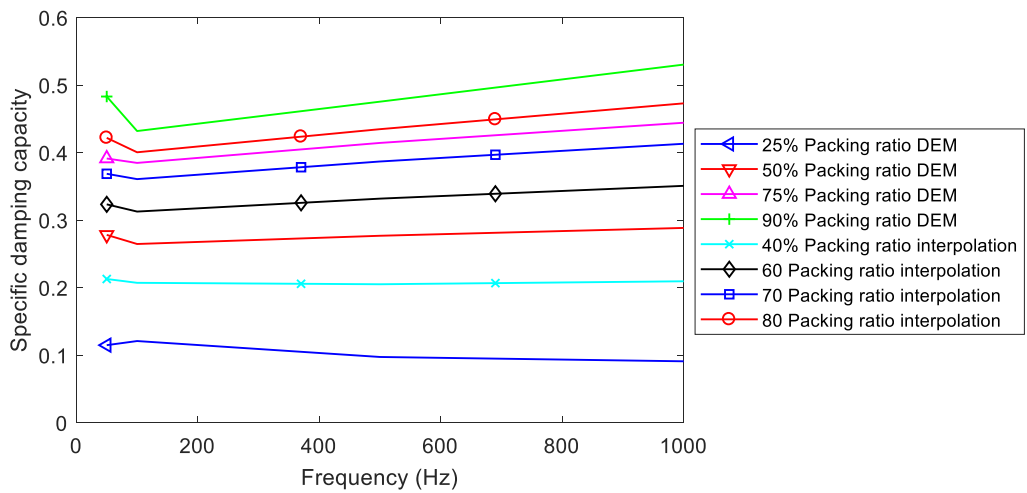


Figure.14. SDC at 10g acceleration level

Conclusions

The dissipation of energy by the damping particles filled in a small coupon of honeycomb is studied with discrete element method and experimentally. The coupon is vibrated with different levels of constant amplitude harmonic acceleration in frequency band of 50Hz - 1000Hz with varying amount of damping particles in the cavity. The energy dissipation is estimated in terms of specific damping capacity and it is found to be dependent on predominantly three parameters: fill fraction, amplitude and frequency of the input acceleration. A multivariate interpolation model of SDC is worked out using ‘pchip’ interpolant. Using the interpolation, SDC is predicted and presented for various combination of the variables. The interpolation function developed herewith for SDC can be used for prediction of structural response of any honeycomb structure treated with damping particles under harmonic, transient excitation loads.

References

- [1] N. Ahmad, R. Ranganath, and A. Ghosal, "Modeling and experimental study of a honeycomb beam filled with damping particles," *Journal of Sound and Vibration*, vol. 391, pp. 20-34, 2017/03/17/ 2017.
- [2] C. Zhang, T. Chen, X. Wang, and Y. Li, "Discrete element method model and damping performance of bean bag dampers," *Journal of Sound and Vibration*, vol. 333, pp. 6024-6037, 2014.
- [3] C. J. Wu, W. H. Liao, and M. Y. Wang, "Modeling of Granular Particle Damping Using Multiphase Flow Theory of Gas-Particle," *Journal of Vibration and Acoustics*, vol. 126, p. 196, 2004.
- [4] M. Saeki, "Analytical study of multi-particle damping," *Journal of Sound and Vibration*, vol. 281, pp. 1133-1144, 2005.
- [5] S. E. Olson, "An analytical particle damping model," *Journal of Sound and Vibration*, vol. 264, pp. 1155-1166, 2003.
- [6] P. A. Cundall and O. D. L. Strack, "A discrete numerical model for granular assemblies," *Géotechnique*, vol. 29, pp. 47-65, 1979.
- [7] Y. Tsuji, T. Tanaka, and T. Ishida, "Lagrangian numerical simulation of plug flow of cohesionless particles in a horizontal pipe," *Powder Technology*, vol. 71, pp. 239-250, 1992.
- [8] K. L. Johnson, *Contact Mechanics*: Cambridge University Press, 1985.
- [9] K. Mao, M. Y. Wang, Z. Xu, and T. Chen, "Simulation and Characterization of Particle Damping in Transient Vibrations," *Journal of Vibration and Acoustics*, vol. 126, p. 202, 2004.
- [10] C. Wong, M. Daniel, and J. Rongong, "Energy dissipation prediction of particle dampers," *Journal of Sound and Vibration*, vol. 319, pp. 91-118, 2009.
- [11] M. Ben Romdhane, N. Bouhaddi, M. Trigui, E. Foltête, and M. Haddar, "The loss factor experimental characterisation of the non-obstructive particles damping approach," *Mechanical Systems and Signal Processing*, vol. 38, pp. 585-600, 2013.